Photochemistry and Photobiology, 2013, 89: 199–207

Modulation of Lipopolysaccharide-Induced NF-κB Signaling Pathway by 635 nm Irradiation *via* Heat Shock Protein 27 in Human Gingival Fibroblast Cells

WonBong Lim[†1], JiSun Kim[†1], SangWoo Kim[1], Sandeep Karna[1], JaeWoong Won[1], Sang Mi Jeon[1], Seo Yeon Kim[1], YooDuk Choi[2], HongRan Choi[1] and OkJoon Kim[*1]

[1]Department of Oral Pathology, School of Dentistry, Dental Science Research Institute, Chonnam National University, Gwangju, Korea
[2]Department of Pathology, Faculty of Medicine, Chonnam National University, Gwangju, Korea

Received 15 February 2012, accepted 6 August 2012, DOI: 10.1111/j.1751-1097.2012.01225.x

ABSTRACT

Heat shock protein-27 (HSP27) is a member of the small HSP family which has been linked to the nuclear factor-kappa B (NF-κB) signaling pathway regulating inflammatory responses. Clinical reports have suggested that low-level light therapy/laser irradiation (LLLT) could be an effective alternative treatment to relieve inflammation during bacterial infection associated with periodontal disease. However, it remains unclear how light irradiation can modulate the NF-κB signaling pathway. We examined whether or not 635 nm irradiation could lead to a modulation of the NF-kB signaling pathway in HSP27-silenced cells and analyzed the functional cross-talk between these factors in NF-κB activation. The results showed that 635 nm irradiation led to a decrease in the HSP27 phosphorylation, reactive oxygen species (ROS) generation, I-κB kinase (IKK)/inhibitor of κB (IκB)/NF-κB phosphorylation, NF-κB p65 translocation and a subsequent decrease in the COX-1/2 expression and prostaglandin (PGE_2) release in lipopolysaccharide(LPS)-induced human gingival fibroblast cells (hGFs). However, in HSP27-silenced hGFs, no obvious changes were observed in ROS generation, IKK/IκB/NF-κB phosphorylation, NF-κB p65 translocation, nor in COX-1/2 expression, or PGE_2 release. This could be a mechanism by which 635 nm irradiation modulates LPS-induced NF-κB signaling pathway *via* HSP27 in inflammation. Thus, HSP27 may play a role in regulating the anti-inflammatory response of LLLT.

INTRODUCTION

In the development and progression of periodontal disease, it has been known that inflammation following *Porphyromonas gingivalis* (*P. gingivalis*) infection leads to the destruction of periodontal tissue and resorption of alveolar bone, ultimately resulting in tooth loss (1,2). A likely candidate for the initiation of a destructive inflammatory response to *P. gingivalis* is lipopolysaccharide (LPS). This bacterial cell wall component is a potent stimulator of the innate host defense system (3). Periodontal disease progression is regulated by the host response to *P. gingivalis*, and there is increasing evidence that nonimmune cells such as human gingival fibroblasts (hGFs) participate in the host response (4). A number of studies report that hGFs express Toll-like receptors (TLR) and CD14, consistent with the finding that these cells respond to LPS (5,6).

NF-κB plays a pivotal role in modulating the cellular signaling mechanism for LPS-induced inflammatory response (7–10). The activation of NF-κB requires phosphorylation of upstream IKK, which contains two catalytic subunits, IKKα and IKKβ (11,12). Upon stimulation with LPS and proinflammatory cytokines, IKK is phosphorylated and activated *via* upstream TGF-β activated kinase 1, resulting in further phosphorylation and degradation of IκB in the ubiquitination pathway (8,13–15). NF-κB then releases from the IκB/NF-κB dimer and translocates from the cytoplasm into the nucleus, inducing further proinflammatory gene expression and inflammatory response. The inhibition of the NF-κB pathway may thus have a potential therapeutic effect in degenerative periodontal diseases.

Given that such a diversity of inducers activate NF-κB *via* the same IKK-dependent pathway, a model has emerged suggesting that all NF-κB activators cause oxidative stress that is mainly responsible for IKK activation and IκB degradation (16,17). This model is based on several observations: most of NF-κB-inducers trigger the formation of reactive oxygen species (ROS), and small heat shock protein 27 (HSP27) is related to ROS. HSP27 is an important member of small HSP family with a variety of functions in health and disease, including ATP-independent chaperone activity in response to the oxidative stress and modulation of inflammation and regulation of actin cytoskeleton dynamics (18–21). For example, when overexpressed in response to various stimuli, HSP27 facilitates phosphorylated IκBα proteasome-mediated proteolysis and enhances NF-κB activity, perhaps accounting for its anti-apoptotic properties (22). Increased levels of HSP27 expression may render tumors more resistant to host defense mechanisms and increase the metastatic potential of tumors. HSP27 activity is regulated by posttranslational modifications such as phosphorylation. HSP27 is rapidly phosphorylated by MAPKAPK2/3 at two or three serine residues in response to various extracellular stresses. Phosphorylation induces the dissociation of HSP27 from high-molecular weight oligomers into tetramers and dimers, resulting in change of some functions of HSP27. HSP27 contributes to

*Corresponding author email: js3894@chonnam.ac.kr (OkJoon Kim)
[†]The first two authors contributed equally to this work.

regulation of, at least in part, NO and ROS production, iNOS expression and TNF-α secretion in activated microglia closely (23–27). HSP27 also plays a negative role in TNF-α-mediated IKK activation and may be involved in down-regulating IKK activity after TNF-α stimulation. A rapid and long-lasting activation of HSP27 in rat primary microglia can be induced by LPS, and the inhibition of c-Jun N-terminal kinase reduces the LPS-induced activity of COX-2, TNF-α, IL-6 and monocyte chemoattractant protein-1 (9). These results have been well summarized in a recent review (16). This research area is still a matter of intense debate, with many conflicting reports.

Several recent reports have suggested that low level red/near infrared light irradiation is an effective alternative treatment that reduces inflammation caused by periodontal disease (28–33). Many physiological studies have reported that low-level laser treatment (LLLT) and light-emitting diode treatment (LEDT) can reduce pain and inflammation and accelerate wound healing (34,35). Some studies have also suggested that irradiation at a wavelength of 635 nm decreases intracellular ROS and mitigates oxidative stress (36–38). It has also been reported that 635 nm irradiation decreases inflammation by inhibiting prostaglandin (PGE_2) production and COX-1 and -2 mRNA expression in *in vitro* and *in vivo* models (34). Although previous studies reported that LLLT or LEDT can reduce inflammation by inhibition of intracellular ROS generation, it has not yet been systemically delineated how light irradiation can modulate the NF-κB pathway in the inflammatory state.

The purpose of the present study was to investigate the effects of 635 nm irradiation on the NF-κB pathway in hGFs in an *in vitro* LPS-induced inflammation model. Considering the mechanisms of NF-κB activation in the inflammatory state, the primary aim was to determine whether or not 635 nm irradiation modulates activation of transcription factor NF-κB *via* the HSP27 signaling pathways. In addition, we wished to examine whether or not 635 nm irradiation led to activation of NF-κB in HSP27-silenced cells and to analyze the functional cross-talk between these factors in NF-κB activation.

MATERIALS AND METHODS

Cell culture. The hGFs were obtained from a healthy 34-year-old adult visiting Chonnam National University Hospital. The gingival tissues were cut finely with scissors and cultured in an alpha minimum essential medium (alpha-MEM; GibcoBRL, MD) supplemented with 10% heat-inactivated fetal bovine serum (Biomeda Co., CA) and antibiotic antimycotic solution (100 U mL penicillin, 0.1 mg mL streptomycin, and 0.25 mg mL amphotericin B; Welgene, Daegu, Korea) at 37°C in a 5% CO_2 humidified chamber. The medium was replaced with fresh medium, and the adherent hGF cells were allowed to reach *ca* 70% confluence. The cells were detached using the trypsin-ethylenediamine tetraacetic acid (trypsin-EDTA: GibcoBRL) solution and plated again (subcultured). After three times with subculture, the experiments were performed in 10 cm dishes (1×10^5 cell mL^{-1}).

Chemical treatments. All chemicals were purchased from Sigma–Aldrich (MO), excepting LPS from *Porphyromonas gingivalis,* obtained from Invivogen (CA). LPS (1 μg mL^{-1}) were added to the cell cultures for inflammatory reaction. BMS-345541 (10 μM, IKK inhibitor) or pyrrolidinedithiocarbamate ammonium (PDTC, 1 μM, NF-κB inhibitor) was added to the cultured cells, simultaneously.

Light source and irradiation. The cultured cell samples were irradiated for 1 h with a light dose of 5 mW cm^{-2} (total energy: 18 J cm^{-2}) and chemically treated simultaneously. A manufactured irradiation tool kit (KNC Wellbeing Co., Korea) was built in a 5% CO_2 humidified chamber held at 37°C. The source of light for irradiation was a continuous-wave light emitting diode (LED; U-JIN LEDs Co., Korea) with a wavelength of 635 nm.

HSP27 silencing by siRNA. The sequence of HSP27 small interfering (si) RNA corresponds to the human HSP27 site (5′-GUCUCAUCGG AUUUUGCAGC-3′: Dharmacon, Lafayette, CO). A scrambled siRNA (5′-CAGCGCUGACAACAGUUUCAU-3′) was used as a control for RNA interference experiments. To treat the siRNA, cells were plated at a density of 4000 cells per 1.9 cm^2, and 24 h later, the cells were treated with each siRNA (5 nM) for 1 day. HiPerFect transfection reagent (Qiagen, IL) was used as a transfection agent for siRNA uptake into cells according to manufacturer's protocol.

Enzyme-linked immunosorbent assay for PGE_2. After the hGFs were incubated with/without the designated reagent for 24 h in the presence or absence of irradiation, the amount of PGE_2 was measured in the supernatants using a commercially available enzyme immunosorbent assay kit (R&D System, MN) according to the manufacturer's protocol. The absorbance of PGE_2 was measured at 450 nm using a colorimetric microplate reader (Biotek, VT).

Luciferase reporter assay. The hGFs were transiently transfected with NF-κB target sequence linked-luciferase reporter plasmid. Transient transfection was carried out using Lipofectamine (Invitrogen) according to the manufacturer's instructions. After transfection, cells were cultured for 24 h, and then irradiations were performed. After irradiation, the cells were exposed to α-MEM with/without designated reagents for the indicated time. Luciferase activity was measured using the Luciferase Assay System (Promega) and detected by luminometer GENios Plus (Tecan Group Ltd., Salzburg, Austria). pCMV-β-gal expression vector was added to each transfection and the β-galactosidase assay was carried out as described previously to normalize the transfection efficiency. Each transfection was performed in triplicate.

Nuclear extract preparations. The hGFs were rinsed in PBS and then collected into the Eppendorf tubes. Solution A (10 mM HEPES, 1.5 mM $MgCl_2$, 10 mM KCl, 0.5 mM DTT, 0.05% NP40 pH 7.9, 0.5 mL) was added and the cells were centrifuged at 805 ***g*** for 10 min at 4°C. The supernatant contained mostly cytoplasmic constituents. To yield a nuclear pellet, 0.4 mL of solution B (5 mM HEPES, 1.5 mM $MgCl_2$, 0.2 mM EDTA, 0.5 mM DTT, 26% glycerol (vol/vol), 300 mM NaCl, pH 7.9) was added, and the tubes were mixed thoroughly and placed on a small rotator shaker for 15 min. Finally, the mixture was centrifuged at 12 000 ***g*** for 3 min in the microcentrifuge. The supernatant containing the proteins from the nuclear extract was removed and transferred carefully to a fresh tube. The nuclear and cytosol extracts were frozen at −80°C in aliquots until Western blotting was done. The protein content of each sample was determined using the BCA protein assay kit (Thermo Scientific, IL).

Western blot analysis. After the hGFs were incubated with/without the designated reagent for the indicated time in the presence or absence of irradiation, the medium was removed and washed twice with PBS. The cell lysates were then prepared in 200 μL of cold lysis buffer (1% NP-40, 50 mM Tris-Hcl, pH 7.5, 150 mM NaCl, 0.02% sodium azide, 150 μg mL^{-1} phenylmethanesulfonyl fluoride, 2 μg mL^{-1} aprotinin, 20 μg mL^{-1} leupeptin and 1 μg mL^{-1} pepstatin A). The cell lysates (30 mg) were separated on a 10% sodium dodecyl sulfate (SDS) polyacrylamide gel and transferred to a polyvinylidene difluoride membrane (Amersham, CA). The membrane was blocked with a blocking solution (5% skim milk in TBST [2.42 g L^{-1} Tris-HCl, 8 g L^{-1} NaCl, 0.1% Tween 20, pH 7.6]) for 30 min and rinsed briefly in TBST. The membrane was incubated overnight at 4°C with the anti-p65-NF-κB antibody (1:1000; Cell signaling, MA), anti-Histone-H1 antibody (1:1000; Santa Cruz, CA), anti-actin antibody (1:1000; Santa Cruz), anti-phospho-HSP27 antibody (1:1000; Santa Cruz), anti-HSP27 antibody (1:1000; Santa Cruz), anti-phospho-IKK α/β antibody (1:1000; Santa Cruz), anti-IKK α antibody (1:1000; Santa Cruz), anti-IKK β antibody (1:1000; Santa Cruz), anti-phospho-IκB antibody (1:1000; Cell signaling), anti-IκB antibody (1:1000), anti-phospho-p65-NF-κB antibody (1:1000; Cell signaling), anti-COX-1 antibody (1:1000; Santa Cruz), and anti-COX-2 antibody (1:1000; Santa Cruz) in 5% non-fat skim milk. After rinsing with TBST, the membrane was incubated for 1 h with anti-rabbit or anti-mouse horseradish peroxidase-conjugated (1:2000) secondary antibody. Finally, the membrane was washed in TBST and the immunoreactivity of the proteins was detected using an enhanced chemiluminescence (ECL) detection kit (Amersham) and determined by densitometric analysis using SCION IMAGE software (Scion Corp., MD).

Immunofluorescence assay. For the detection of intracellular location of NF-κB p65 subunit, hGFs were seeded on four-well chamber slide. After 1 h of experiment, the cells were fixed in cold 3.8% paraformalde-

hyde, membrane-permeabilized by exposure to 0.2% Triton X-100 in cold PBS for 30 min, and blocked in 5% bovine serum albumin (BSA; in PBST [0.2% Tween-20 in PBS]) at room temperature for 30 min. The rabbit anti-NF-κB p65 subunit (1:200, diluted in PBST containing 5% BSA) was then used as the primary antibody and incubated with the cells for 2 h at room temperature. After sufficient washes with PBST, cells were incubated with FITC-labeled goat anti-rabbit IgG antibody (10 μg mL^{-1} diluted in PBST containing 5% BSA) for 1 h at room temperature in a dark place, and washed with PBST for 10 min. Cells were then stained with 5 μg mL^{-1} of DAPI for 30 min at 37°C in a dark place, followed by sufficient washes with PBS. Stained cells were analyzed using a confocal microscope (Carl Zeiss, Oberkochen, Germany), excitation wavelength 490 nm and emission wavelength 540 nm for FITC, excitation wavelength 360 nm and emission wavelength 450 nm for DAPI.

Detection of total ROS formation. Total ROS were assayed using 2′,7′-dichlorodihydrofluorescein diacetate (H_2DCF-DA; Sigma–Aldrich) as described in the previous report (36). To visualize intracellular ROS, cells were checked immediately after experimental treatment. The hGFs grown on chamber slides were incubated with 20 μM H_2DCF-DA for 20 min. Cells were washed with PBS containing 10 mM glucose, and DCF fluorescence intensity was monitored using a confocal microscope (Carl Zeiss) set at the excitation and emission wavelengths of 488 and 525 nm, respectively.

To measure the intracellular ROS levels, the cells were washed with PBS containing 10 mM glucose and treated with 10 μM H_2DCFDA for 20 min. The treated cells were detached using trypsin-EDTA solution, and the ROS level was analyzed by flow cytometry (Beckman Coulter) using 485-nm excitation and 530-nm emission filters.

Statistical analysis. All experiments were carried out in triplicate. Data are expressed as means ± SD. The results were subjected to an analysis of the variance (ANOVA) using SPSS for Windows version 12.0 (SPSS V12.0K; SPSS Inc., Chicago, IL) to analyze the differences. Null hypotheses of no difference were rejected if *P*-values were less than 0.05.

RESULTS

Effect of 635 nm irradiation on PGE_2 release, NF-κB activation and p-65 translocation in IKK or NF-κB-inactivated hGFs

To investigate the effect of 635 nm irradiation on IKK or NF-κB inhibitor-induced inflammation in hGFs, PGE_2 release was assayed in LPS-treated hGFs with or without BMS-345541 or PDTC (39). Treatment of hGFs with LPS led to an increase in PGE_2 production up to 280 pg mL^{-1}, whereas 635 nm irradiation led to a significant decrease in the PGE_2 level in the LPS-treated hGFs (Fig. 1a). In the BMS-345541 or PDTC-treated hGFs, no obvious changes in the PGE_2 level were detected after 635 nm irradiation.

To investigate the effect of 635 nm irradiation on NF-κB activity, hGFs were transiently transfected with pNF-κB-Luc vector (Fig. 1b). NF-κB activity was enhanced 2.0–2.5 fold compared to that in the control following 1 and 24 h treatment of LPS. However, the increase in NF-κB-dependent luciferase activity was significantly suppressed by 635 nm irradiation at 1 and 24 h. The irradiations with 635 nm in BMS-345541 or PDTC-treated hGFs had little effect on NF-κB activity compared to that in nonirradiated hGFs.

Stimulated NF-κB can induce its translocation into the nucleus where it binds to the promoter regions of several proinflammatory genes. Treatment with LPS significantly increased NF-κB p65 translocation into the nucleus (Fig. 1c). However, in the presence of 635 nm irradiation, the elevatory nuclear translocation of NF-κB was inhibited in LPS-activated hGFs, thereby showing that the activation of NF-κB was blocked by 635 nm irradiation. An additional inhibitory effect of 635 nm irradiation on NF-κB p65 translocation into the nucleus was seen in the BMS-345541-treated hGFs. This effect was not observed in the PDTC-treated cells. These findings were supported by immunofluorescence assay data *via* detection of intracellular location of NF-κB p65 subunit (Fig. 1d). Irradiation with 635 nm could inhibit nuclear translocation of NF-κB p65 in LPS-activated hGFs in the presence or absence of BMS-345541. No obvious changes in nuclear translocation of NF-κB p65 after 635 nm irradiation were observed in LPS-activated hGFs in the presence of PDTC.

Effect of 635 nm irradiation on HSP27 phosphorylation in LPS-treated hGFs

In Fig. 2a, irradiation with 635 nm could significantly inhibit phosphorylation of HSP27 in LPS-induced hGFs. This suggests that 635 nm irradiation could suppress HSP27 phosphorylation in LPS-induced hGFs, and decrease stimulation downstream of HSP27 activation.

To clarify whether or not the HSP27 activation is involved in the NF-κB pathway, knockdown of HSP27 by small interference RNA (siRNA) was performed in hGFs. Western blot analysis confirmed low expression levels of HSP27 in HSP27 siRNA - transfected cells compared with control (Fig. 2b).

Effect of 635 nm irradiation on ROS generation in HSP27 siRNA-induced hGFs

On confocal microscopy, 635 nm irradiation led to a decrease in DCF fluorescence indicating intracellular ROS production in control siRNA-treated hGFs in the presence of LPS (Fig. 3a). On the other hand, treatment of HSP27-siRNA induced the DCF fluorescence increase in hGFs over all. There were no obvious changes between LPS-treated group and LPS with 635 nm irradiation-treated group.

Flow cytometry showed DCF fluorescence decreased from 71.7 to 3.2 with 635 nm irradiation in control siRNA-treated hGFs in the presence of LPS (Fig. 3b). However, 635 nm irradiation could not lead to a decrease in DCF fluorescence in HSP27 siRNA-treated hGFs in the presence of LPS. These results indicated that 635 nm irradiation did not affect the intracellular ROS level in HSP27-silenced hGFs.

Effect of 635 nm irradiation on IKK, IkB, NF-kB phosphorylation and NF-kB translocation in HSP27 siRNA-induced hGFs

To investigate the effect of 635 nm irradiation on LPS-induced activation of IKK and degradation of IκB in HSP27-silenced hGFs, the phosphorylated and total protein expression of IKK α/β (two catalytic subunits) and IκB were detected by western blotting. A significant decrease in phosphorylated IκB and IKK levels was seen with 635 nm irradiation in the presence of LPS in control siRNA-treated hGFs (Fig. 4a,b). However, 635 nm irradiation could not decrease the phosphorylation of IκB and IKK in HSP27 siRNA-treated hGFs.

In Figs. 4c and d, the effect of 635 nm irradiation on phosphorylation of NF-κB p65 subunit at serine 276 and translocation into the nucleus is compared between control and HSP27 siRNA-treated hGFs in the presence or absence of LPS. In control

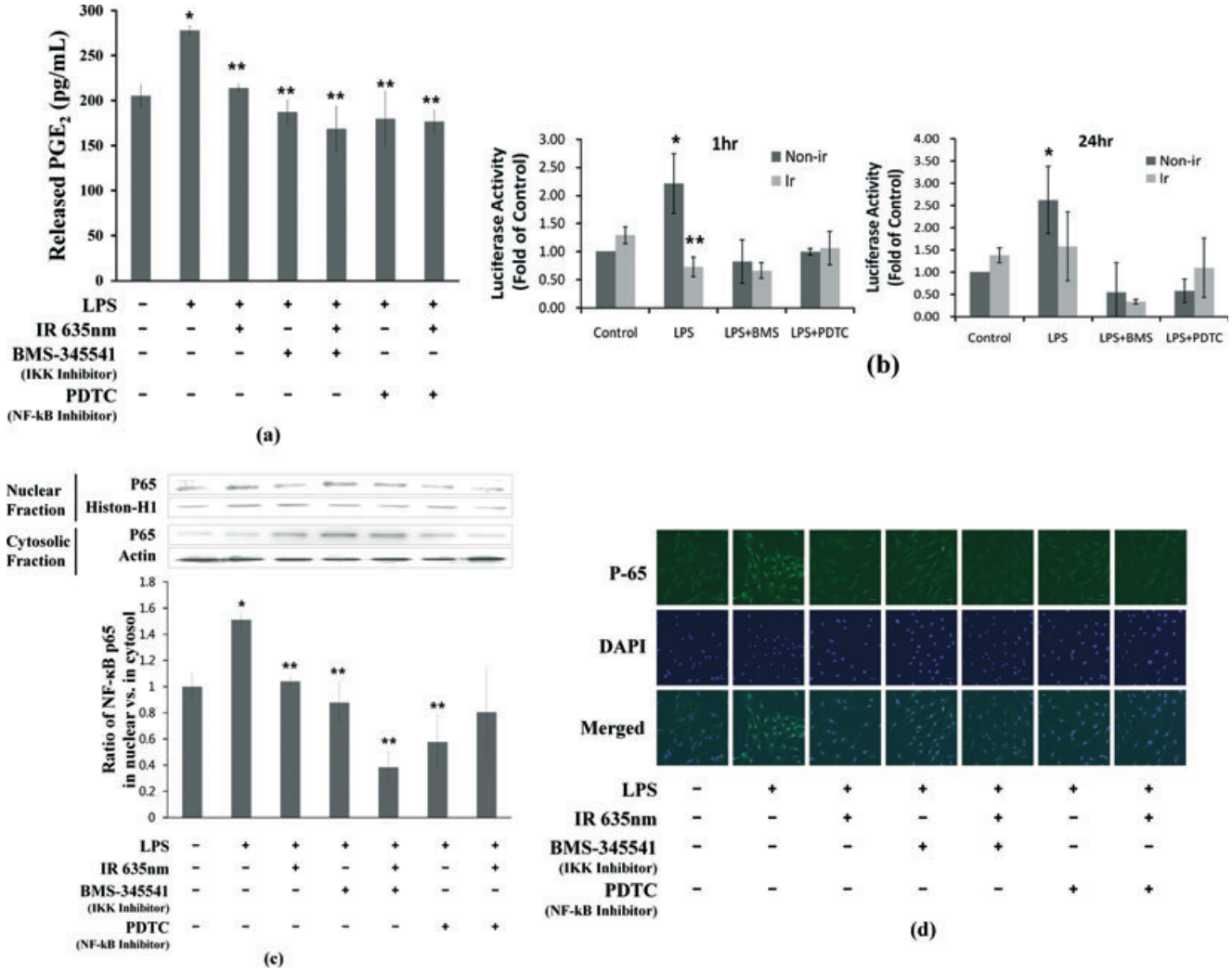

Figure 1. Effects of 635 nm irradiation on BMS-345541 (IKK inhibitor, 10 μM) or PDTC(NF-κB inhibitor, 1 μM)-induced PGE_2 release, NF-kB activation and p-65 translocation in *P. gingivalis* lipopolysaccharide(LPS)-treated hGFs. (a) Release of PGE_2 was measured from the culture medium at 24 h, and these were processed for analysis by ELISA. Significant differences were seen at $^*P < 0.05$ compared with control and $^{**}P < 0.05$ compared with LPS. (b) The BMS-345541 or PDTC-treated hGFs were transiently transfected with pNF-κB-Luc reporter gene and then treated with 1 μg mL^{-1} LPS in the presence or absence of 635 m irradiation for 1–24 h. Luciferase activities were determined as described in the "Materials and Methods" section. The results are expressed as means ± SD of triplicate tests. Significant differences were seen at $^*P < 0.05$ compared with control. (c) The p-65 nuclear translocation was analyzed by western blotting in cytosolic and nuclear fractions at 1 h. Histone-H1 from the nuclear fraction or actin from cytosol were employed to load the same protein concentration as the loading controls. Densitometric analysis of p-65 in the cytosolic and nuclear fractions represents the mean ratio ±SD of three separate experiments. Significant differences were seen at $^*P < 0.05$ compared with control and $^{**}P < 0.05$ compared with LPS. (d) Confocal microscopy observation of nuclear translocation of NF-κB p65 subunit. Immunofluorescence images were acquired by using a confocal microscope stained for NF-κB p65 subunit (green) and nucleus (blue). All magnifications are 200×. All the size bar is 20 μm.

siRNA-induced treated hGFs, irradiation with 635 nm led to a decrease in the elevatory phosphorylation and nuclear translocation of NF-κB in the presence of LPS, showing that the activation of NF-κB was blocked by 635 nm irradiation. No inhibitory effect of 635 nm irradiation on NF-κB phosphorylation and translocation was seen in HSP27 siRNA-treated hGFs.

To confirm the involvement of HSP27 along with 635 nm irradiation in the NF-κB pathway, the intracellular location of NF-κB p65 subunit was detected using immunofluorescence assay (Fig. 4e). Irradiation with 635 nm could inhibit nuclear translocation of NF-κB p65 in LPS-inuced hGFs in the presence of control siRNA. No obvious changes in nuclear translocation of NF-κB p65 were observed with 635 nm irradiation in the presence of HSP27 siRNA.

Effect of 635 nm irradiation on COX-1/2 expression and PGE_2 release in HSP27 siRNA-induced hGFs

To delineate the anti-inflammatory mechanism of 635 nm irradiation in association with HSP27, we examined whether or not 635 nm irradiation could lead to a decrease in COX-1/2 expression and PGE_2 release in HSP27 siRNA-treated hGFs. The 635 nm irradiation resulted in a marked decrease in COX-1/2 expression and PGE_2 release in control siRNA-treated hGFs in the presence of LPS (Fig 5a,b). However, 635 nm irradiation had no effect on COX-1/2 expressions or PGE2 release in the HSP27 siRNA-treated cells. Therefore, it seems that the expression of COX-1/2 and PGE_2 release is decreased by 635 nm irradiation only dependent upon HSP27.

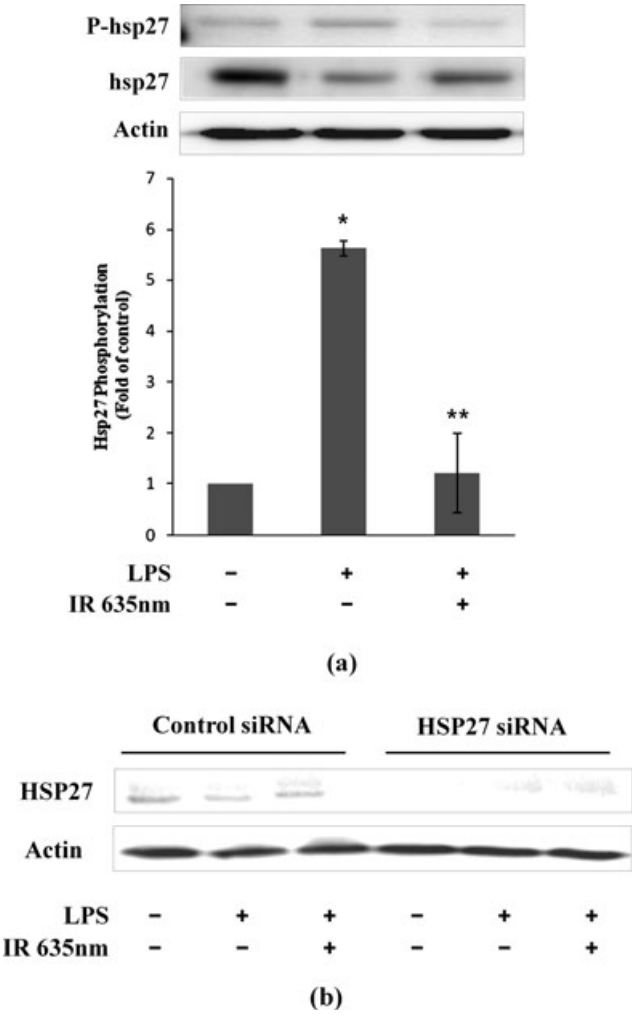

Figure 2. Phosphorylation of HSP27 and suppression of HSP27 protein expression by treatment with HSP27 siRNA in *P. gingivalis* lipopolysaccharide(LPS)-treated hGFs. (a) Western blot assay of hGFs exposed to LPS (1 μg mL^{-1}) for 1 h with or without irradiation was performed. Cells were processed for analysis of HSP27 phosphorylation by western blot utilizing anti-phospho HSP27. The membranes were denuded and antibodies were directed against nonphosphorylated forms of HSP27 as controls. The results obtained were similar in the three separate experiments; the mean ± SD was obtained by densitometry, as shown in the graphic analysis. Significant differences were seen at $*P < 0.05$ compared to control and at $**P < 0.05$ compared with LPS. (b) The HSP27 protein expression in HSP27-silenced/HSP27-knockout hGFs is represented by western blot assay. The hGFs were treated with 5 nM HSP27 siRNA or control siRNA for 24 h. The cells were exposed to LPS (1 μg mL^{-1}) for 1 h with or without irradiation. Cells were processed for analysis of HSP27 by western blot utilizing anti-phospho HSP27. Membranes were denuded and actin was employed to load the same protein concentration as a loading control.

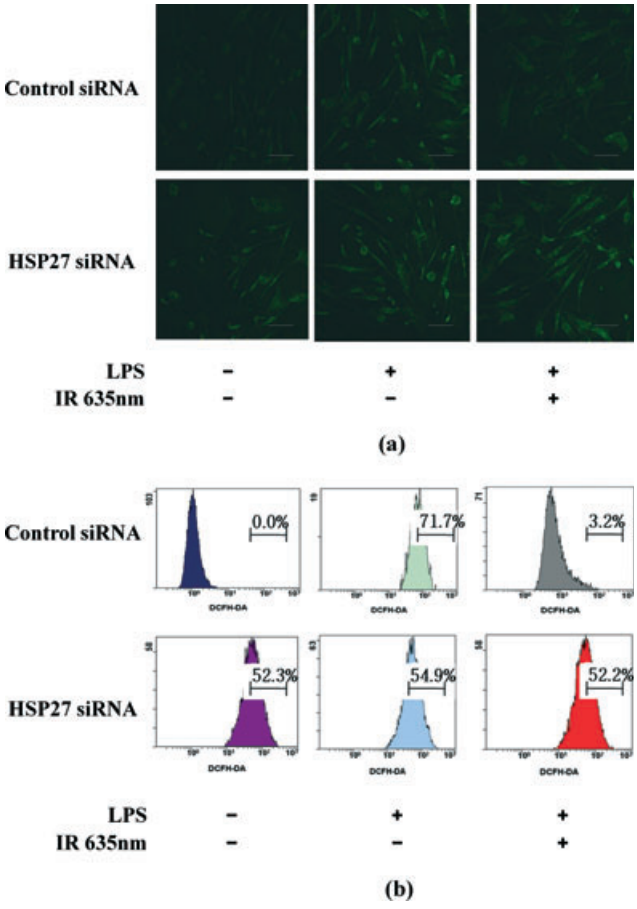

Figure 3. The effect of 635 nm irradiation on ROS generation in HSP27 siRNA or control siRNA-treated hGFs in the presence of LPS. (a) Green fluorescence of DCF-DA, indicating intracellular ROS formation, was detected by a confocal microscopy. All magnifications are 200×. All the size bar is 20 μm. (b) The DCF fluorescence distribution is represented by flow cytometry histograms (*x*-axis: log of the fluorescence intensity from 10^0 to 10^4; *y*-axis: cell number from 0 to 100).

DISCUSSION

LLLT has gained considerable recognition for its anti-inflammatory properties (40,41). In a previous study, LLLT with 635 nm could reduce inflammation as effectively as indomethacin or ibuprofen, well-established anti-inflammatory agents (34). Irradiation with 635 nm was shown to decrease intracellular ROS, which mediate $cPLA_2$, $sPLA_2$ and COX-2 expression, and inhibit the release of PGE_2. For this intracellular PGE_2 synthesis, NF-κB plays a pivotal role in modulating the cellular signaling mechanism. Although previous studies have shown that 635 nm irradiation acts as an inflammation inhibitor, the mechanism by which irradiation with 635 nm regulates activation of NF-κB-mediated inflammatory responses has not been described until now. Therefore, a further goal of this study was to explore the mechanisms underlying the anti-inflammatory effect of 635 nm irradiation involving the NF-κB pathway. In resting cells, NF-κB exists in the cytosol in a dimeric form of NF-κB and IκB, an associated inhibitory protein. Administration of LPS *in vitro* or *in vivo* results in the activation of the NF-κB upstream signaling regulator IKK, which further induces phosphorylation and subsequent degradation of IκB (11,42). The free NF-κB then translocates into the nucleus and enhances the transcription of proinflammatory genes (8). In the present study, 635 nm irradiation in LPS-induced hGFs significantly suppressed the release of PGE_2. Moreover, 635 m irradiation suppressed the activation and nuclear translocation of NF-κB p65 subunit, and thereby showed that the anti-inflammatory effect of 635 nm irradiation may be related to its ability to inhibit the NF-κB signaling pathway. However, when NF-κB activation is blocked by a selective inhibitor, 635 nm irradiation did not affect PGE_2 production. In IKK-blocked hGFs, 635 nm irradiation could not affect the activity and the nuclear translocation of NF-κB p65.

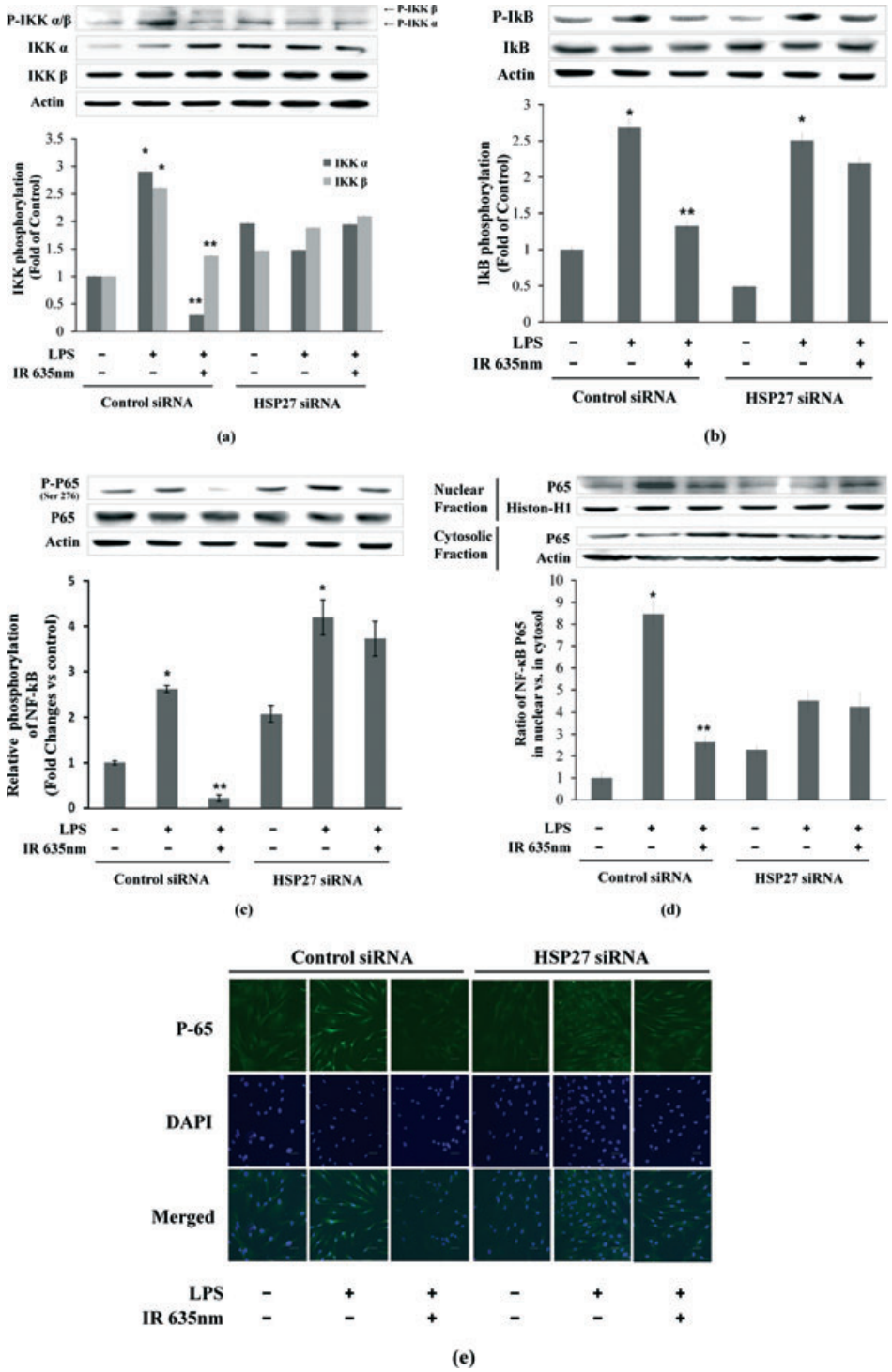

Figure 4. The effect of 635 nm irradiation on activation of NF-kB pathway in HSP27 siRNA-treated hGFs in the presence of LPS. (a) Phosphorylation of IKK α/β in HSP27 siRNA or control siRNA-treated hGFs. The hGFs were treated with 5 nM HSP27 siRNA or control siRNA for 24 h. The cells were exposed to LPS (1 μg mL^{-1}) for 1 h with or without irradiation. Cells were processed for analysis of IKK α/β phosphorylation by western blot utilizing anti-phospho IKK α/β. The membranes were denuded and antibodies were directed against nonphosphorylated forms of IKK α/β as controls. The results obtained were similar in the three separate experiments; the mean ± SD was obtained by densitometry, as shown in the graphic analysis. Significant differences were seen at $^{*}P < 0.05$ compared with control and at $^{**}P < 0.05$ compared with LPS. (b) Phosphorylation of IkB in HSP27 siRNA or control siRNA-treated hGFs. (c) Phosphorylation of NF-κB p65 in HSP27 siRNA or control siRNA-treated hGFs. (d) Nuclear translocation of the p65 in HSP27 siRNA or control siRNA-treated hGFs. The nuclear translocation of NF-kB subunit was analyzed by western blotting in the cytosolic and nuclear fractions. Histone-H1 from the nuclear fraction or actin from cytosol were employed to load the same protein concentration as the loading controls. Densitometric analysis of p65 in the cytosolic and nuclear fractions represent the mean ratio ± SD from three separate experiments (e) Confocal microscopy observation of nuclear translocation of NF-κB p65 subunit in HSP27 siRNA or control siRNA-treated hGFs. Immunofluorescence images were acquired by using a confocal microscope after staining for NF-κB p65 subunit (green) and nucleus (blue). All magnifications are 200×. All the size bar is 20 μm.

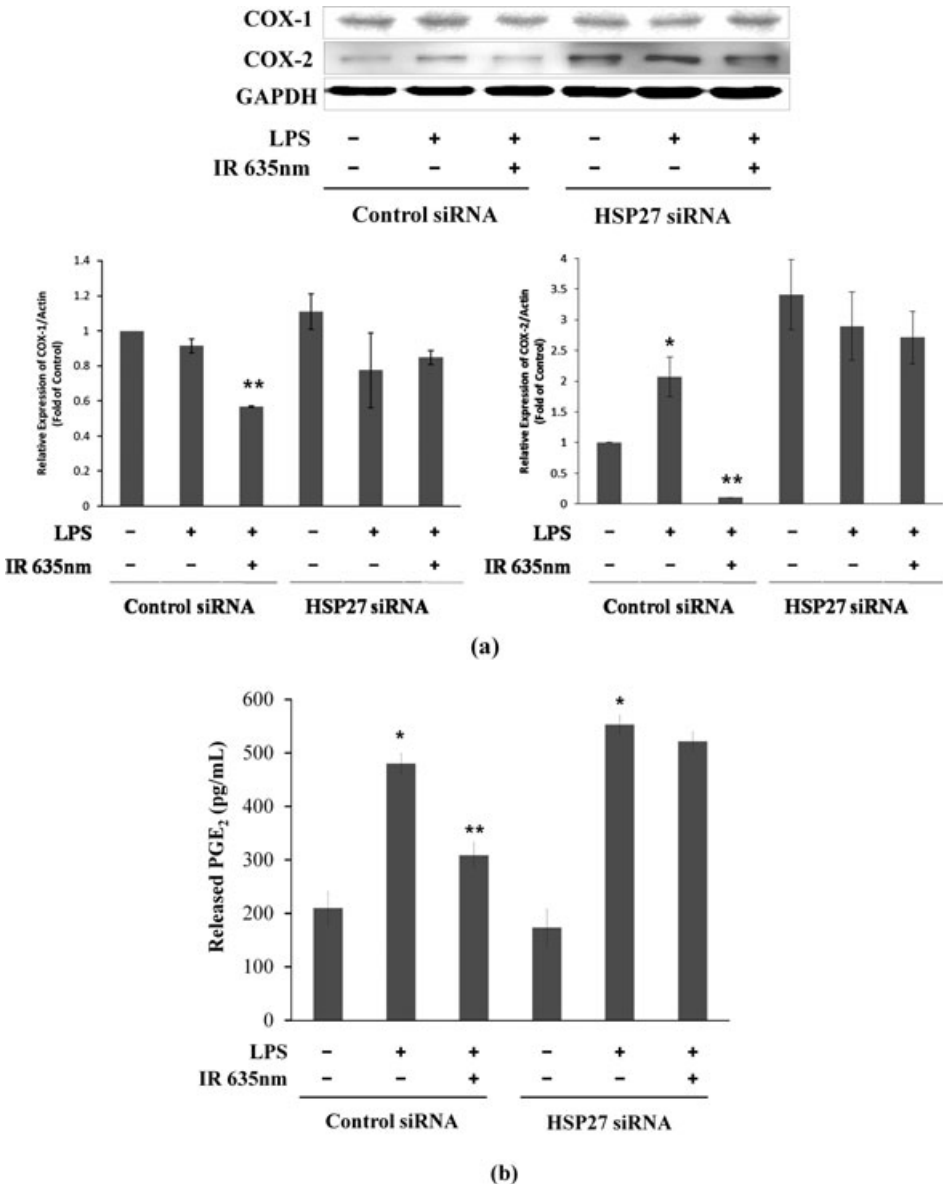

Figure 5. Effects of 635 nm irradiation on cylooxygenase-1/2 (COX-1/2) expression and PGE_2 release in HSP27 siRNA-treated hGFs in the presence of LPS. (a) The COX-1/2 protein expression in HSP27-silenced/HSP27-knockout hGFs was analyzed by western blot assay. The hGFs were treated with 5 nM HSP27 siRNA or control siRNA for 24 h. And then, the cells were exposed to LPS (1 μg mL^{-1}) for 24 h with or without irradiation. Cells were processed for analysis of COX-1/2 by western blot utilizing anti-COX-1/2. Membranes were denuded and actin was employed to load the same protein concentration as a loading control. Densitometric analysis of COX-1/2 represents the mean ratio ± SD from three separate experiments. Significant differences were seen at $*P < 0.05$ compared with control and $**P < 0.05$ compared with LPS. (b) Release of PGE_2 was measured from the culture medium at 24 h, and these were processed for analysis by ELISA.

These data suggest that 635 nm irradiation might play a pivotal role in modulating inflammatory reaction, and its inhibitory effect on NF-κB activation is dependent on the upstream regulator of IKK.

HSP27 has been suggested as the factor which could be affected by 635 nm irradiation leading to activation of NF-κB-mediated inflammatory responses. It is recognized that HSP27 is an important modulator of NF-κB activation through IKK, and its response is affected by various intra/extracellular stimuli such as redox potential (43). HSP27 is a stress-responsive protein associated with reduced stress response in the inflammatory state (24,44). HSP27 becomes rapidly phosphorylated at three serine sites (Ser^{15}, Ser^{78} and Ser^{82}) in response to cytotoxic stress or exposure to cytokines and mitogen (18,26). Under unstimulated conditions, HSP27 exists as a high-molecular weight aggregate that dissociates after phosphorylation. The capacity of HSP27 seems to be determined by the phosphorylation status, and our results show that 635 nm irradiation inhibits phosphorylation of HSP27 in LPS-induced hGFs, indicating that phosphor-HSP27 is decreased by 635 nm irradiation. The phosphorylation of HSP27 occurs very early during stress and is tightly regulated. This phosphorylation is caused by the triggering of a highly specific heat shock-sensing pathway (26). Some studies have suggested that HSP27 contributes to maintenance of redox homeostasis and mitochondrial stability in the

inflammatory state, with increased expression of HSP27 during stress response associated with the redox balance from excessive ROS generation in cytotoxic stress (45). Since HSP27 deletion in this study leads the ROS generation in presence or absence of LPS in hGFs, HSP27 therefore plays a critical role in reduction of oxidative stress through ROS decrease.

ROS is involved in the initiation and progression of inflammation. It has been reported that 635 nm irradiation showed not only an anti-inflammatory effect by suppression of COX-2 activation but also an ROS-scavenging effect by constitutive suppression of ROS in arachidonic acid-induced hGFs (34). Therefore, we examined whether or not 635 nm irradiation could interact with ROS generation in HSP27-silenced hGFs. In the presence of LPS, 635 nm irradiation could not decrease the intracellular ROS generation in HSP27-silenced hGFs by HSP27 siRNA treatment indicating the critical role of HSP27 under 635 nm irradiation of decreasing ROS during inflammation.

Oxidative stress due to increased ROS production is thought to be a major factor contributing to the activation of NF-κB signaling pathway during inflammation. Activation of the ROS pathway is held to be initiated by interactions with membrane lipids (46). These reactions generate free radicals and stimulate a cascade that may include other mediators often implicated in LPS-induced inflammation. The ROS-induced cascade appears to culminate in the rise of HSP27 phosphorylation and an increase in IKK-IkB phosphorylation. The modulation of NF-κB by low level light irradiation may well be related to the anti-oxidative, ROS-scavenging activity, consonant with its ability to suppress NF-κB activation (47). In the experiments presented in this study, a significant decrease in phosphorylated IκB, IKK and NF-κB levels by 635 nm irradiation was seen in control siRNA-treated hGFs, resulting in inhibition of NF-κB p65 translocation into the nucleus. However, 635 nm irradiation could not decrease phosphorylation of IκB, IKK and NF-κB in HSP27-silenced hGFs and no obvious changes in nuclear translocation of NF-κB p65 by 635 nm irradiation were detected. This indicated that 635 nm irradiation could lead to a decrease in ROS generation, IKK and IK-B phosphorylation, sequentially, through HSP27 in the inflammatory state, thereby leading to reduced nuclear translocation of NF-κB. These results might partially explain the specific regulation of ROS generation by 635 nm irradiation through HSP27 in the NF-κB activation pathway. It has been shown that NF-κB modulation by 635 nm irradiation through HSP27 is required for down regulation of pro-inflammatory gene expression in hGFs. This suggests that HSP27 is essential for 635 nm irradiation–induced down regulation of COX-2 expression and inhibition of PGE_2 secretion due to its effect on NF-κB.

In conclusion, we here report the novel findings that 635 nm irradiation attenuates LPS-induced NF-κB activation in hGFs *via* HSP27 leading to inhibition of the intracellular ROS generation and IKK, IκB phosphorylation (Fig. 6). In addition, inhibition of the inflammatory reaction by 635 nm irradiation can be an effective approach to prevent inflammatory responses in LPS-induced NF-κB activation pathway. This suggests that the role of HSP27 in 635 nm irradiation-induced decrease in inflammation is crucial for regulating LPS-induced inflammation during bacterial infection in periodontal disease and HSP27 can be used as a potential target for anti-inflammatory therapy with LLLT.

Acknowledgement—This research was supported by the Basic Science Research Program through the National Research Foundation of Korea (NRF) funded by the Ministry of Education, Science and Technology (2010-0007676).

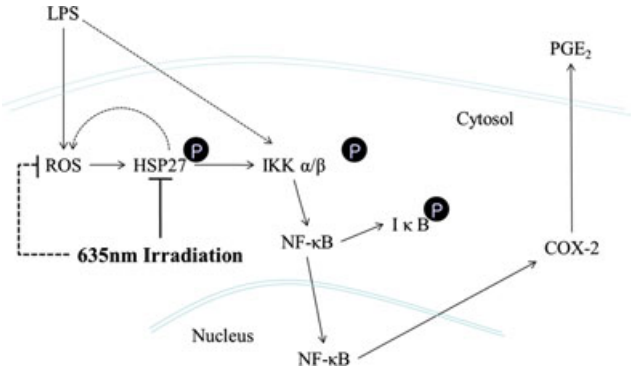

Figure 6. A proposed model of LPS-induced activation of NF-κB and PGE_2 release through ROS-HSP27-IKK mediated pathway, along with the possible points of 635 nm irradiation involvement. The increase of ROS by LPS stimulation leads to phosphorylation of HSP27 and IKK $\alpha\beta$, and hence promotes COX-2 expression and PGE_2 release by increase of NF-κB translocation to the nucleus. 635 nm irradiation is shown to decrease the phosphorylation of HSP27, IKK α and NF-κB translocation, finally resulting in a decreased expression of COX-2 and release of PGE_2.

REFERENCES

1. Asai, Y., M. Hashimoto, H. M. Fletcher, K. Miyake, S. Akira and T. Ogawa (2005) Lipopolysaccharide preparation extracted from *Porphyromonas gingivalis* lipoprotein-deficient mutant shows a marked decrease in Toll-like receptor 2-mediated signaling. *Infect. Immun.* **73**, 2157–2163.
2. Socransky, S. S., A. D. Haffajee, M. A. Cugini, C. Smith and R. L. Kent Jr. (1998) Microbial complexes in subgingival plaque. *J. Clin. Periodontol.* **25**, 134–144.
3. Kocgozlu, L., R. Elkaim, H. Tenenbaum and S. Werner (2009) Variable cell responses to *P. gingivalis* lipopolysaccharide. *J. Dent. Res.* **88**, 741–745.
4. Seymour, G. J. and E. Gemmell (2001) Cytokines in periodontal disease: Where to from here? *Acta Odontol. Scand.* **59**, 167–173.
5. Applequist, S. E., R. Wallin and H. G. Ljunggren (2002) Variable expression of Toll-like receptor in murine innate and adaptive immune cell lines. *Int. Immunol.* **14**, 1065.
6. Gutierrez-Venegas, G., M. Jimenez-Estrada and S. Maldonado (2007) The effect of flavonoids on transduction mechanisms in lipopolysaccharide-treated human gingival fibroblasts. *Int. Immunopharmacol.* **7**, 1199–1210.
7. Pomerantz, J. L. and D. Baltimore (2002) Two pathways to NF-kappaB. *Mol. Cell* **10**, 693–695.
8. Li, X. and G. R. Stark (2002) NFkappaB-dependent signaling pathways. *Exp. Hematol.* **30**, 285–296.
9. Zeng, K.-W., H. Fu, G.-X. Liu and X.-M. Wang (2010) Icariin attenuates lipopolysaccharide-induced microglial activation and resultant death of neurons by inhibiting TAK1/IKK/NF-κB and JNK/p38 MAPK pathways. *Int. Immunopharmacol.* **10**, 668–678.
10. Lawrence, T. (2009) The nuclear factor NF-κB pathway in inflammation. *Cold Spring Harb. Perspect. Biol.* **1**, a001651.
11. Israel, A. (2009) The IKK complex, a central regulator of NF-κB activation. *Cold Spring Harb. Perspect. Biol.* **2**, a000158.
12. Ferreiro, D. U. and E. A. Komives (2010) Molecular mechanisms of system control of NF-κB signaling by IκBα. *Biochemistry* **49**, 1560–1567.
13. Brasier, A. R. (2010) The nuclear factor-κB-interleukin-6 signalling pathway mediating vascular inflammation. *Cardiovasc. Res.* **86**, 211–218.
14. Majdalawieh, A. and H.-S. Ro (2010) Regulation of IκBα function and NF-κB signaling: AEBP1 is a novel proinflammatory mediator in macrophages. *Mediators Inflamm.* **2010**, 1–27.
15. Yamauchi, J., S. Takai, R. Matsushimanishiwaki, Y. Hanai, T. Doi, H. Kato, S. Ogura, K. Kato, H. Tokuda and O. Kozawa (2007) (−)

-Epigallocatechin gallate inhibits prostaglandin D2-stimulated HSP27 induction *via* suppression of the p44/p42 MAP kinase pathway in osteoblasts. *Prostaglandins Leukot. Essent. Fatty Acids* **77**, 173–179.
16. Gloire, G., S. Legrandpoels and J. Piette (2006) NF-κB activation by reactive oxygen species: Fifteen years later. *Biochem. Pharmacol.* **72**, 1493–1505.
17. Song, Y. S., M.-S. Kim, H.-A. Kim, B.-I. Jung, J. Yang, P. Narasimhan, G. S. Kim, J. E. Jung, E.-H. Park and P. H. Chan (2010) Oxidative stress increases phosphorylation of IκB kinase-α by enhancing NF-κB-inducing kinase after transient focal cerebral ischemia. *J. Cereb. Blood Flow Metab.* **30**, 1265–1274.
18. Liu, J., S. Hong, Z. Feng, Y. Xin, Q. Wang, J. Fu, C. Zhang, G. Li, L. Luo and Z. Yin (2010) Regulation of lipopolysaccharide-induced inflammatory response by heat shock protein 27 in THP-1 cells. *Cell. Immunol.* **264**, 127–134.
19. Arrigo, A. P., S. Simon, B. Gibert, C. Kretz-Remy, M. Nivon, A. Czekalla, D. Guillet, M. Moulin, C. Diaz-Latoud and P. Vicart (2007) Hsp27 (HspB1) and alphaB-crystallin (HspB5) as therapeutic targets. *FEBS Lett.* **581**, 3665–3674.
20. Clark, J. I. and P. J. Muchowski (2000) Small heat-shock proteins and their potential role in human disease. *Curr. Opin. Struct. Biol.* **10**, 52–59.
21. Sun, Y. and T. H. MacRae (2005) The small heat shock proteins and their role in human disease. *FEBS J.* **272**, 2613–2627.
22. Parcellier, A., E. Schmitt, S. Gurbuxani, D. Seigneurin-Berny, A. Pance, A. Chantome, S. Plenchette, S. Khochbin, E. Solary and C. Garrido (2003) HSP27 is a ubiquitin-binding protein involved in I-kappaBalpha proteasomal degradation. *Mol. Cell. Biol.* **23**, 5790–5802.
23. Hadchity, E., M.-T. Aloy, C. Paulin, E. Armandy, E. Watkin, R. Rousson, M. Gleave, O. Chapet and C. Rodriguez-Lafrasse (2009) Heat shock protein 27 as a new therapeutic target for radiation sensitization of head and neck squamous cell carcinoma. *Mol. Ther.* **17**, 1387–1394.
24. Guo, K., N. Kang, Y. Li, L. Sun, L. Gan, F. Cui, M. Gao and K. Liu (2009) Regulation of HSP27 on NF-κB pathway activation may be involved in metastatic hepatocellular carcinoma cells apoptosis. *BMC Cancer* **9**, 100.
25. Kim, M. K., S. W. Chung, D. H. Kim, J. M. Kim, E. K. Lee, J. Y. Kim, Y. M. Ha, Y. H. Kim, J.-K. No and H. S. Chung (2010) Modulation of age-related NF-κB activation by dietary zingerone *via* MAPK pathway. *Exp. Gerontol.* **45**, 419–426.
26. Shin, J.-K., Y.-T. Jeong, H.-C. Jo, M.-Y. Kang, I.-S. Chang, J.-C. Baek, J.-K. Park, S.-A. Lee, J.-H. Lee, W.-S. Choi and W.-Y. Paik (2009) Increased interaction between heat shock protein 27 and mitogen-activated protein kinase (p38 and extracellular signal-regulated kinase) in pre-eclamptic placentas. *J. Obstet. Gynaecol. Res.* **35**, 888–894.
27. Wang, Z., R. Gao, Y. Huang, B. Tian and Y. Zhou (2009) Effects of mitogen-activated protein kinase signal pathway on heat shock protein 27 expression in human lens epithelial cells exposed to sodium salicylate *in vitro*. *J. Huazhong Univ. Sci. Technolog. Med. Sci.* **29**, 377–382.
28. Faria Amorim, J. C., G. R. D. Sousa, L. D. B. Silveira, R. A. Prates, M. Pinotti and M. S. Ribeiro (2006) Clinical study of the gingiva healing after gingivectomy and low-level laser therapy. *Photomed. Laser Ther.* **24**, 588–594.
29. Sun, G. and J. Tuner (2004) Low-level laser therapy in dentistry. *Dent. Clin. North Am.* **48**, 1061–1076.
30. Koleva, S. (2008) 29 Gingival crevicular fluid IL-1 [beta] and PGE2 in periodontal health, disease and after LLLT. *Photodiagn. Photodyn. Ther.* **5**, S11.
31. de Almeida, P., R. A. Lopes-Martins, S. S. Tomazoni, J. A. Silva Jr, T. de Carvalho Pde, J. M. Bjordal and E. C. Leal Junior (2011) Low-level laser therapy improves skeletal muscle performance, decreases skeletal muscle damage and modulates mRNA expression of COX-1 and COX-2 in a dose–dependent manner. *Photochem. Photobiol.* **87**, 1159–1163.
32. Esteves Junior, I., I. B. Masson, C. T. Oshima, A. P. Paiotti, R. E. Liebano and H. Plapler (2012) Low-level laser irradiation, cyclooxygenase-2 (COX-2) expression and necrosis of random skin flaps in rats. *Lasers Med. Sci.* **27**, 655–660.
33. Pires, D., M. Xavier, T. Araujo, J. A. Silva Jr, F. Aimbire and R. Albertini (2011) Low-level laser therapy (LLLT; 780 nm) acts differently on mRNA expression of anti- and pro-inflammatory mediators in an experimental model of collagenase-induced tendinitis in rat. *Lasers Med. Sci.* **26**, 85–94.
34. Lim, W., S. Lee, I. Kim, M. Chung, M. Kim, H. Lim, J. Park, O. Kim and H. Choi (2007) The anti-inflammatory mechanism of 635 nm light-emitting-diode irradiation compared with existing COX inhibitors. *Lasers Surg. Med.* **39**, 614–621.
35. Gao, X. and D. Xing (2009) Molecular mechanisms of cell proliferation induced by low power laser irradiation. *J. Biomed. Sci.* **16**, 4.
36. Lim, W., J. H. Kim, E. Gook, J. Kim, Y. Ko, I. Kim, H. Kwon, H. Lim, B. Jung, K. Yang, N. Choi, M. Kim, S. Kim, H. Choi and O. Kim (2009) Inhibition of mitochondria-dependent apoptosis by 635-nm irradiation in sodium nitroprusside-treated SH-SY5Y cells. *Free Radic. Biol. Med.* **47**, 850–857.
37. Fillipin, L. I., J. L. Mauriz, K. Vedovelli, A. J. Moreira, C. G. Zettler, O. Lech, N. P. Marroni and J. Gonzalez-Gallego (2005) Low-level laser therapy (LLLT) prevents oxidative stress and reduces fibrosis in rat traumatized Achilles tendon. *Lasers Surg. Med.* **37**, 293–300.
38. Fujimaki, Y., T. Shimoyama, Q. Liu, T. Umeda, S. Nakaji and K. Sugawara (2003) Low-level laser irradiation attenuates production of reactive oxygen species by human neutrophils. *J. Clin. Laser Med. Surg.* **21**, 165–170.
39. Nuutinen, U., A. Ropponen, J. Eeva, M. Eray, R. Pellinen, J. Wahlfors and J. Pelkonen (2009) The effect of microenvironmental CD40 signals on TRAIL- and drug-induced apoptosis in follicular lymphoma cells. *Scand. J. Immunol.* **70**, 565–573.
40. Walker, M. D., S. Rumpf, G. D. Baxter, D. G. Hirst and A. S. Lowe (2000) Effect of low-intensity laser irradiation (660 nm) on a radiation-impaired wound-healing model in murine skin. *Lasers Surg. Med.* **26**, 41–47.
41. Whelan, H. T., R. L.. Smits Jr, E. V. Buchman, N. T. Whelan, S. G. Turner, D. A. Margolis, V. Cevenini, H. Stinson, R. Ignatius, T. Martin, J. Cwiklinski, A. F. Philippi, W. R. Graf, B. Hodgson, L. Gould, M. Kane, G. Chen and J. Caviness (2001) Effect of NASA light-emitting diode irradiation on wound healing. *J. Clin. Laser Med. Surg.* **19**, 305–314.
42. Karin, M. and M. Delhase (2000) The I kappa B kinase (IKK) and NF-kappa B: Key elements of proinflammatory signalling. *Semin. Immunol.* **12**, 85–98.
43. Arrigo, A. P., W. J. Firdaus, G. Mellier, M. Moulin, C. Paul, C. Diaz-latoud and C. Kretz-remy (2005) Cytotoxic effects induced by oxidative stress in cultured mammalian cells and protection provided by Hsp27 expression. *Methods*, **35**, 126–138.
44. Bhattacharyya, S., P. K. Dudeja and J. K. Tobacman (2009) ROS, Hsp27, and IKKβ mediate dextran sodium sulfate (DSS) activation of IκBa, NFκB, and IL-8. *Inflamm. Bowel Dis.* **15**, 673–683.
45. Kamada, M., A. So, M. Muramaki, P. Rocchi, E. Beraldi and M. Gleave (2007) Hsp27 knockdown using nucleotide-based therapies inhibit tumor growth and enhance chemotherapy in human bladder cancer cells. *Mol. Cancer Ther.* **6**, 299–308.
46. Bhattacharyya, S., P. K. Dudeja and J. K. Tobacman (2008) Lipopolysaccharide activates NF-kappaB by TLR4-Bcl10-dependent and independent pathways in colonic epithelial cells. *Am. J. Physiol. Gastrointest. Liver Physiol.* **295**, G784–G790.
47. Chen, A. C.-H., Y.-Y. Huang, P. R. Arany and M. R. Hamblin (2009) Role of reactive oxygen species in low level light therapy. *Proc. SPIE* **7165**, 716502–1–716502–11.